



## LJMU Research Online

García Plaza, E, Chen, X and Ait Ouarab, L

**Abrasive Feature Related Acoustic Emission in Grinding**

<http://researchonline.ljmu.ac.uk/id/eprint/11321/>

### Article

**Citation** (please note it is advisable to refer to the publisher's version if you intend to cite from this work)

**García Plaza, E, Chen, X and Ait Ouarab, L Abrasive Feature Related Acoustic Emission in Grinding. Xplore, IEEE International conference on automation and computing. (Accepted)**

LJMU has developed [LJMU Research Online](http://researchonline.ljmu.ac.uk) for users to access the research output of the University more effectively. Copyright © and Moral Rights for the papers on this site are retained by the individual authors and/or other copyright owners. Users may download and/or print one copy of any article(s) in LJMU Research Online to facilitate their private study or for non-commercial research. You may not engage in further distribution of the material or use it for any profit-making activities or any commercial gain.

The version presented here may differ from the published version or from the version of the record. Please see the repository URL above for details on accessing the published version and note that access may require a subscription.

For more information please contact [researchonline@ljmu.ac.uk](mailto:researchonline@ljmu.ac.uk)

<http://researchonline.ljmu.ac.uk/>

# *Abrasive Feature Related Acoustic Emission in Grinding*

E. García Plaza<sup>1</sup>, X. Chen<sup>2</sup>, L.A Ouarab<sup>2</sup>

<sup>1</sup>Higher Technical School of Industrial Engineering, Department Applied Mechanics & Engineering of Projects, University of Castilla-La Mancha, Avda. Camilo José Cela, s/n, 13005 Ciudad Real, Spain.

<sup>2</sup>Advanced Manufacturing Technology Research Laboratory, General Engineering Research Institute, Liverpool John Moores University, Liverpool L3 3AF, UK.

**Abstract**—Grinding monitoring enables the online supervision of crucial aspects of the process, such as tool state, surface quality, and dimensional accuracy; and possesses a great advantage over traditional post-process quality control techniques by reducing costs and inspection times. Such an advantage relies on a good interpretation of monitored signals in relation to grinding behaviours. This paper presents an experimental study on acoustic emission (AE) features in abrasive grinding scratch experiments. The acoustic emission signals are analysed in both the time and frequency domains. The results show that the signal feature extraction in the frequency domain gives excellent indication in correlation to the surface creation with different abrasive geometrical characteristics. The AE features in the frequency range between 0 and 200 kHz show good correlation with the characteristics of interaction between abrasive and workpiece in scratching tests and could be an ideal data source for the online monitoring of surface creation in grinding processes.

**Keywords**- *acoustic emission; signal feature extraction; abrasive scratch, frequency analysis.*

## I. INTRODUCTION

An online monitoring system for machining processes could have remarkable impacts on a CNC machine tools system in reducing manufacturing cost and time in the product inspections, and avoiding the need for post-process quality control [1][2]. Online monitoring techniques allow the real time evaluation of crucial aspects of the machining processes, such as tool condition [3] [4], chatter [5], surface finish [6][7], chip formation [8], surface damage [9] [10], and so on. In order to provide effective information with online monitoring techniques, the selection of adequate sensors, signal processing methods together with predictive techniques should be optimised according to the specific parameters under analysis. A broad range of sensors have been used in machining process monitoring, including dynamometers, accelerometers and acoustic emission sensors [2]. For online process monitoring, different signal processing methods in time domain and frequency domain have been applied, i.e., time direct analysis (TDA) [6], singular spectrum analysis (SSA) [11], Fourier transform [6], and wavelet transform [12], and so on. Considering correlating features of the parameters under study, several predictive techniques have been applied in many researches, i.e., the multivariate regression [13], the artificial neural networks [6] and the support vector machines (SVM) [4].

Of all machining processes, grinding is one of commonly used processes for finishing operations that produce workpieces with close tolerance and high surface quality. In grinding, the wheel surface topography is an important aspect to evaluate due to the abrasive grain shapes change continuously, which directly affect the ground component quality. In recent years, online monitoring techniques have been extensively applied to grinding process to monitor important aspects, such as tool wear [14], surface finish [15], surface damage [9], and so on. Nguyen et al. [15] developed a model to predict the abrasive wear and the surface finish using cutting force signals. The signals were processed in time and frequency domain and the wear and the surface finish were predicted using adaptive neural fuzzy inference system, Gaussian process regression and Taguchi methods. Similarly, Tang et al. [16] developed a mathematical model of grinding forces to characterise the surface topography of the workpieces.

One of the most important signals used in grinding process monitoring has been acoustic emission (AE), which is defined as an elastic wave propagation in the bandwidth between 20 and 2000 kHz due to material molecular displacements under stresses [17]. In grinding, the AE signal represents many important aspects of grinding, such as: grain and bounding ruptures in the wheel, workpiece chipping, cracks, elastic and plastic deformation, phase transformation, and so on. Thus, AE signal has been used to characterise different physical performances of grinding processes. Boaron and Weingaertner [3] analysed acoustic emission signals in both the time and frequency domain for evaluation of the topographic characteristics of a fused aluminium oxide grinding wheel. The method was based on the detection of the effective width of the grinding wheel with an instrumented diamond tip. Rameshkumar et al. [4] registered the acoustic signal in grinding operation to predict the wear level of the grinding wheel. The acoustic emission was analysed in time domain using different features such as root mean square, amplitude, ring-down count, average signal level. By using machine-learning techniques, for example, decision tree, artificial neural network, and support vector machine, they could estimate if the wheel was sharp or dull. Using the same way, Liao [12] developed a grinding wheel condition monitoring method based on acoustic emission wavelet packet transform to estimate the wheel sharpness or dullness. Later, Liao [18] developed a model based on the analysis of acoustic emission signal using autoregressive

modelling and discrete wavelet decomposition to classify the state of grinding wheel. Liu et al. [9] [10] determined the wavelet packet transform was an ideal signal processing method to evaluate the acoustic emission signal and to extract features correlated to the grinding burn phenomena. Chiu and Guao [19] constructed an SVM model for the state classification of CBN grinding with featured data from acoustic emission signal. Dias et al. [20] proposed a new methodology to predict and detect the surface quality and the dimensional errors by acoustic emission in centreless grinding process. The acoustic emission was processed in both the frequency and the time-frequency domain by fast Fourier transform and wavelet analysis, respectively

Most of the studied in grinding process monitoring have used the acoustic emission signal to classify the wear level of the grinding wheel. However, the direct relationship between the acoustic emission and the surface quality of the machined workpiece have been studied in a less extent and more research in this field is needed. In this study, the objective is to monitor grinding surface creation based on the acoustic emission signal acquired during grinding scratch tests.

To evaluate the acoustic emission signal two signal feature extraction methods were applied, i.e, the time domain analysis (TDA) and the frequency analysis with the fast Fourier transform (FFT). The whole bandwidth of the acoustic emission signal was analysed to determine the frequency ranges with more information correlated with grinding process. In order to correlate the signal characterization parameters with the surface creation, multiple regression predictive models were developed. All predictive models were analysed independently for each workpiece materials without direct information of abrasive grains in the models as the data for the model development is based exclusively on the acoustic emission signals.

## II. EXPERIMENTAL PROCEDURE

The experimental procedure was carried out by abrasive scratch experiments on a numerical control grinding machine XR 610 VMC Heidenhein, using abrasive cutting tools assembled to a rotating steel wheel (see Fig. 1a). Five different types of diamond abrasives were used for the cutting tools. The workpiece materials selected for testing were zirconia and sapphire. Each test was carried out in dry conditions, with a cutting speed ( $V_s$ ) of 1 m/s, a downward feed rate ( $V_w$ ) of 1000 mm/min and a cutting depth ( $a_e$ ) of 1  $\mu$ m. The cutting spindle rotational speed was 238 rpm. In each machining trial, the acoustic emission (AE) was registered using a Physical Acoustics WD sensor mounted as near as possible to the cutting zone with a sampling frequency ( $f_s$ ) of 2 MHz. As show in Fig. 1b, each scratch surface was measured using a Bruker interferometer and the deepest cut ( $D$ ) and its width of cut ( $W$ ) were evaluated. The parameter selected to characterize the surface creation was the ratio  $W/D$ . The registered acoustic emission signal in each test was subdivided into scratch n signals (Fig. 1c). This subdivision enabled the direct correlation between the acoustic emission signals and the experimental values of the  $W/D$  parameter.

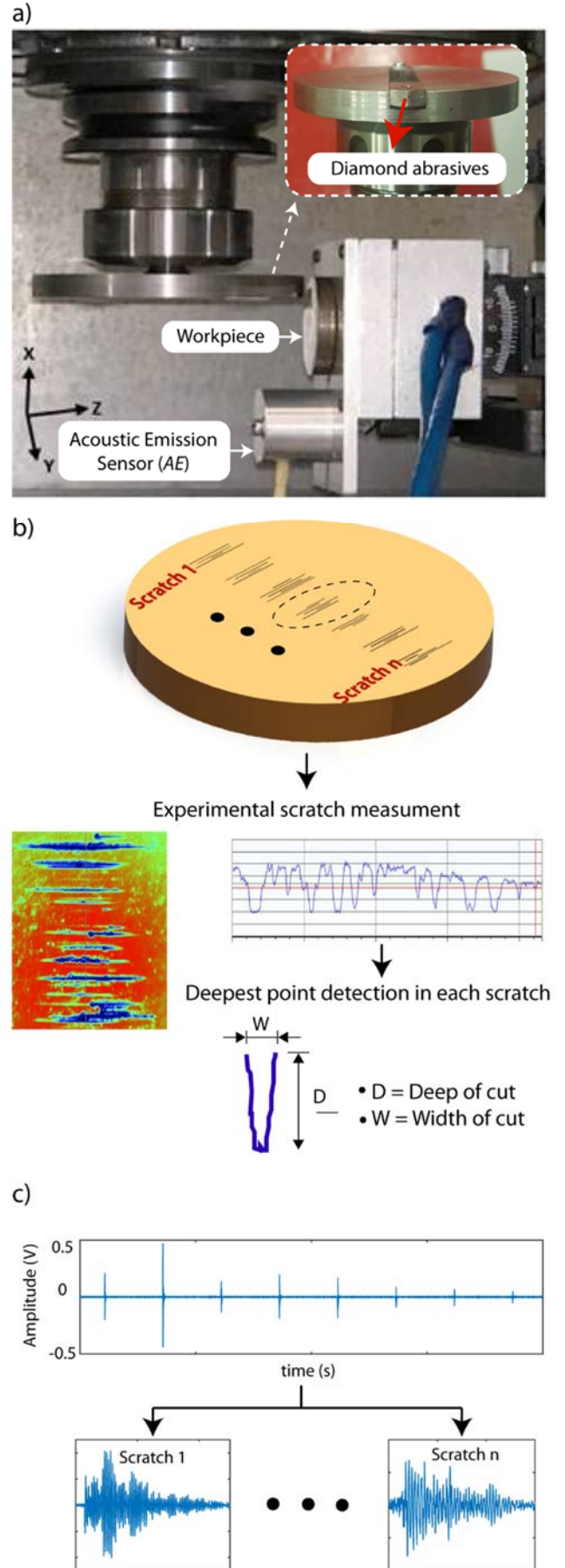


Figure 1. Experimental set-up.

### III. METHODOLOGY

Fig. 2 shows the methodology applied in this study to determine the optimum signal feature extraction for the monitoring of surface creation in relation to  $W/D$  parameter. The first step (a) involved the application of the TDA and FFT signal processing methods to the acoustic emission signal. The next step (b) was statistical signal characterization by evaluating the features shown in Table I. In step (c), signal feature parameters were correlated with the  $W/D$  parameter using predictive regression models. Finally, (d) an exhaustive analysis of signal feature extraction method was carried out to build and assess the targeted predictive models based on multivariable polynomial regression method.

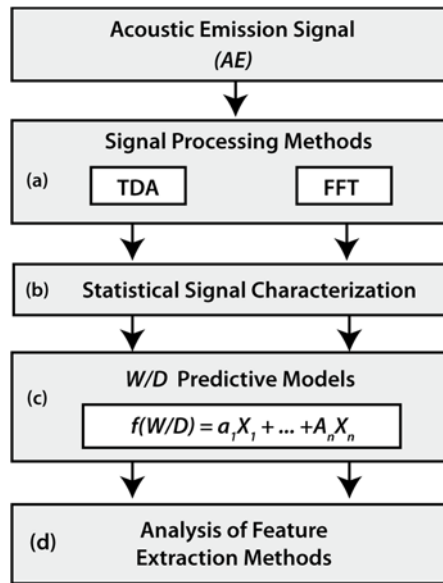


Figure 2. Methodology.

TABLE I. STATISTICAL FEATURE EXTRACTION OF ACOUSTIC EMISSION SIGNAL.

FEATURES	TIME DOMAIN	FREQUENCY DOMAIN
Root mean square	$RMS$	$RMS^f$
Standard deviation	$SD$	$SD^f$
Maximum amplitude	-	$A^f$
Peak to peak amplitude	$PP$	-
Kurtosis	$K$	$K^f$
Skewness	$S$	$S^f$
Energy	$E$	$E^f$
Entropy	$SE$	$SE^f$
Mean	$X$	$X^f$
Frequency of maximum	-	$F^f$

Where the superscript  $f$  indicates the frequency range ( $f_1, \dots, f_n$ )

All of the models obtained were diagnosed by analysing atypical values, multicollinearity, independence and normality of the residuals, homoscedasticity, and

hypothesis contrast tests. The predictive models were built using stepwise regression method to obtain only variables statistically significant at 90 % of confidence (p-value). Predictive models were assessed in three ways. Firstly, the goodness of fit to experimental data was evaluated using the adjusted determination coefficient (adjusted R-squared,  $R^2_{adj}$ ). Secondly, the sum of squares type III and the p-values [21] were studied in order to determine the variables more correlated with the  $W/D$  parameter. Finally, the goodness of fit was evaluated by the graphical representation of the experimental values of  $W/D$  versus the predicted values with the predictive model.

### IV. RESULT AND DISCUSSION

#### A. Time domain analysis (TDA)

The TDA method directly analyses the raw  $AE$  signals in the time domain, with no transformation or decomposition. This method provides fast signal processing at a low analytical-computational cost, making it suitable for real time applications. The efficacy of the TDA method mainly depends on the type of the machining process, the registered signal and the process parameter under assessment. In many occasions, working directly with the time signal provide an adequate signal characterization, however, in some cases, this method cannot extract significant distinctive information, which often is hidden or masked in the signal itself. The signal feature extraction using TDA method in this study is based on the parameters showed in Table 1.

Considering the models built by TDA method to estimate  $W/D$  parameter in relation to  $AE$  signal features, Table 2 depicts the determination coefficient ( $R^2_{adj}$ ) of the regression models, the type III sum of squares [21] and the p-values for the significant characterization parameters. For both sapphire and zirconia materials, it can be observed that the obtained predictive models give very poor results in correlation to the parameter  $W/D$ . The model for sapphire expressed only 10.6% of the variability of the experimental data, and the model for zirconia expressed the 25.5 %. This implies that the signal feature extraction method in time domain (TDA) failed to achieve an adequate signal characterisation.

TABLE II. SIGNIFICANT PARAMETERS OF THE SAPPHIRE AND ZIRCONIA PREDICTIVE MODELS FOR THE TDA METHOD.

Sapphire			Zirconia		
$R^2_{adj} = 10.6\%$			$R^2_{adj} = 25.25\%$		
Features	SS Type III	p-Value	Features	SS Type III	p-Value
$K$	4871	0.018	$RMS$	1611.5	0.001
$Error$	31942	-	$E$	949.6	0.010
-	-	-	$Error$	5066.6	-

The analysis of the goodness of fit to the experimental data of the TDA method are shown in Fig. 3, which revealed that TDA method failed to provide adequate signal feature extraction for the prediction of  $W/D$  parameter.

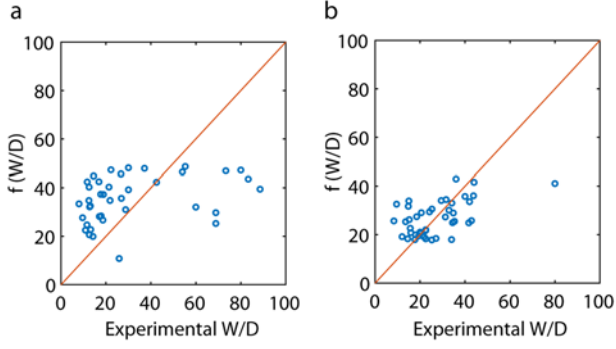


Figure 3. Estimated values vs experimental values of the parameter  $W/D$  for TDA method. a) Sapphire, b) Zirconia.

### B. Frequency analysis (FFT)

In the machining process monitoring, Fourier transform analysis provides the information of the frequency spectrum of monitored signals. For the succession  $x[i]$  the discrete Fourier transform (DFT) was defined by (1):

$$X_k = \sum_{i=0}^{N-1} x_i e^{-j \left( \frac{2\pi k i}{N} \right)}, \quad k = 0, 1, 2, \dots, (N-1) \quad (1)$$

The main restriction of (1) is its high computational cost, due to requires the calculus of  $N$  multiplications of the term  $x_i e^{-j(2\pi k i / N)}$  for each of the  $N$  values of  $X_k$ , in other words, this algorithm entails the calculation of approximately  $N^2$ . Thus, for high frequency sample signals, as acoustic emission signal is, the use of this algorithm may not be a suitable processing method. To overcome this drawback, the DFT is implemented by using the algorithm with the highest computational efficiency denominated fast Fourier transform (FFT), which reduces the number of operations to  $N \log_2 N$ .

Typical power spectrums of  $AE$  signal for both the sapphire and zirconia materials are shown in the top of Fig. 4 with similar behaviours in all diamond scratch tests. The  $AE$  spectrum reaches the maximum amplitude at approximately 35 kHz. After that frequency, the power spectrum gradually decreases until around 400 kHz, then, a few feature peaks of power spectrum were found between 450 and 600 kHz.

According to the previous analysis, it can be seen that relevant spectrum frequency range is around 0-600 kHz. The frequency analysis of  $AE$  signal was undertaken with a complete analysis of the bandwidth 0-600 kHz (see Fig. 4). It should be noted, that the total bandwidth under analysis entails certain frequency ranges with significant information fails to be adequately characterized, thus, the bandwidth 0-600 kHz was discretized into six independent frequency ranges of 100 kHz each (Fig. 4). Secondly, the analysis was focused on the lower frequencies due to the high power spectrum of this area. As shown in Fig. 5, this analysis was assessed in the frequency range 0-200 kHz. To achieve a precise signal characterization at lower frequencies, each frequency range was fractioned into independent intervals of 10 kHz.

1) *Analysis of frequency range 0-600 kHz:* The Table 3 depicts the results of the regression models for estimating  $W/D$  parameter by the processing of the  $AE$  signal in the bandwidth 0-600 kHz with FFT method, for both the sapphire and zirconia materials. Table 3 shows the determination coefficient ( $R^2_{adj}$ ), the frequency ranges, the type III sum of squares and the p-values for the significant characterization parameters.

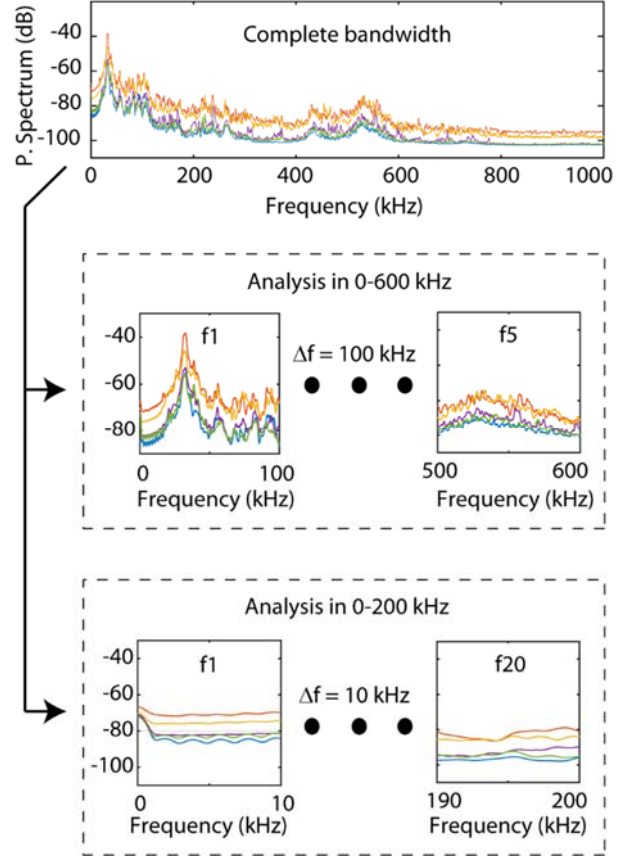


Figure 4. Frequency ranges for  $AE$  signal analysis

As it was mentioned in Table I, the superscript of the features indicates the frequency range of this variable, for example, the feature  $X^{12}$  indicate the arithmetic mean of the FFT in the frequency range 100-200 kHz. It can be observed that both materials, obtained predictive models with very poor results, having little impact on the parameter  $W/D$ . The model for sapphire explained the 33.62% of the variability of the experimental data, and the model for zirconia only the 18.52 %, which indicated a very poor correlation to  $W/D$  parameter.

The analysis of the goodness of fit to the experimental data of the FFT method in the entire bandwidth are shown in Fig. 5. The results were quite similar to TDA analysis, where the predictive models for both materials obtained poor results. The model for sapphire (Fig. 5a) overestimated the data in most of the experimental data, and the model for zirconia (Fig. 5b) obtained better results with homogeneous distribution, but with higher deviation in many data. This implies the analysis of the bandwidth 0-600 kHz in intervals of 100 kHz is not effective to extract

significant information of *AE* signal correlated with *W/D* parameter.

TABLE III. SIGNIFICANT PARAMETERS OF THE SAPPHIRE AND ZIRCONIA PREDICTIVE MODELS FOR THE FFT METHOD IN 0-600 KHZ.

Sapphire			Zirconia		
$R^2_{adj} = 33.62\%$			$R^2_{adj} = 18.52\%$		
Features	SS Type III	p-Value	Features	SS Type III	p-Value
$\chi^2$	1824	0.089	$\chi^{f1}$	901.6	0,016
$S^{f3}$	6218	0.003	$E^{f5}$	491.2	0.070
$SE^{f3}$	2982	0.031	Error	5522.9	-
$E^{f6}$	5957	0.003	-	-	-
Error	22051	-	-	-	-

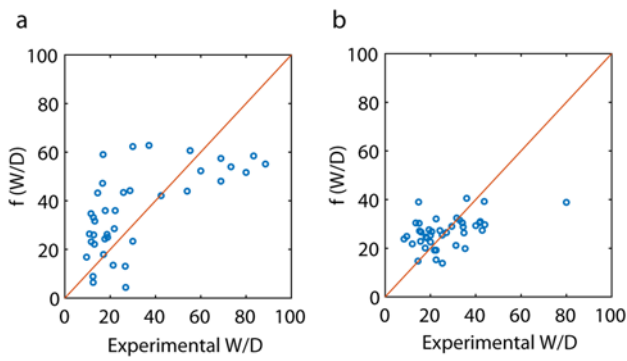


Figure 5. Estimated values vs experimental values of the parameter *W/D* for FFT method in 0-600 kHz. a) Sapphire, b) Zirconia.

2) *Analysis of frequency range 0-200kHz*: Table 4 shows the significant features for the predictive models obtained in the frequency range 0-200 kHz. It can be observed that the determination coefficient for both models the sapphire and zirconia dramatically increase, with  $R^2_{adj}$  values of 95.84% and 90.07%, respectively. For the sapphire model, a broad number of the analysed frequency bands showed significant information correlated with the parameter *W/D*. The ranges f4 (30-40 kHz) provided the most significant feature of the model ( $A^{f4}$ ) with the highest sum of square. This frequency range correspond with the higher power spectrum of the *AE* signal (see Fig 4). The next frequency bands providing high values of sum of square were in decreasing order f9 ( $S^{f9}$ ), f3 ( $A^{f3}$ ), f20 ( $SE^{f20}$ ), f14 ( $K^{f14}$ ), f16 ( $SE^{f16}$ ). The rest of significant frequency ranges provided also information but into a less extent. For the model of zirconia, similar to sapphire, a broad number of the analysed frequency ranges provided information correlated with the *W/D* parameter. However, in contrast with the model for sapphire, higher differences in the sum of squares of the significant features were not found for zirconia; the maximum difference is reached in the range f16 ( $F^{f16}$ ), where a value slightly higher than that in the rest of the variables.

TABLE IV. SIGNIFICANT PARAMETERS OF THE SAPPHIRE AND ZIRCONIA PREDICTIVE MODELS FOR THE FFT METHOD IN 0-200 KHZ.

Sapphire			Zirconia		
$R^2_{adj} = 95.48\%$			$R^2_{adj} = 90.07\%$		
Feat.	SS Type III	p-Value	Feat.	SS Type III	p-Value
$A^{f3}$	8779.6	0.000	$K^{f1}$	556.9	0.000
$S^{f3}$	876.8	0.000	$SE^{f2}$	166.3	0.005
$A^{f4}$	10797.7	0.000	$S^{f5}$	221.6	0.001
$\chi^{f5}$	302.9	0.011	$K^{f6}$	353.6	0.000
$A^{f6}$	2754.1	0.000	$F^{f6}$	169.7	0.004
$F^{f6}$	4189.0	0.000	$E^{f9}$	389.0	0.000
$SD^{f8}$	2140.2	0.000	$SD^{f10}$	493.6	0.000
$S^{f9}$	9021.8	0.000	$RMS^{f14}$	655.5	0.000
$K^{f11}$	3324.4	0.000	$\chi^{f14}$	922.0	0.000
$K^{f13}$	2149.6	0.000	$K^{f15}$	491.3	0.000
$K^{f14}$	6879.5	0.000	$F^{f15}$	176.4	0.004
$SE^{f16}$	5887.5	0.000	$F^{f16}$	1472.2	0.000
$A^{f17}$	883.9	0.000	$SD^{f19}$	824.3	0.000
$E^{f18}$	214.2	0.030	$A^{f20}$	366.8	0.000
$F^{f18}$	1570.6	0.000	$\chi^{f20}$	787.2	0.000
$SE^{f20}$	7163.6	0.000	$F^{f20}$	804.8	0.000
Error	1013.6	-	Error	431.6	-

The analysis of the correlations of the estimated data versus the experimental data for the FFT method in the 0-200 kHz frequency band (Fig. 6) revealed the model for zirconia had an even distribution in all of the *W/D* parameter ranges, with no bias and a very strong correlation (see Fig 6b). The model obtained for sapphire (Fig 6a), in spite of having higher determination coefficient than zirconia model, showed a higher deviation in all of frequency ranges with under-estimation of *W/D* values between 10 and 20.

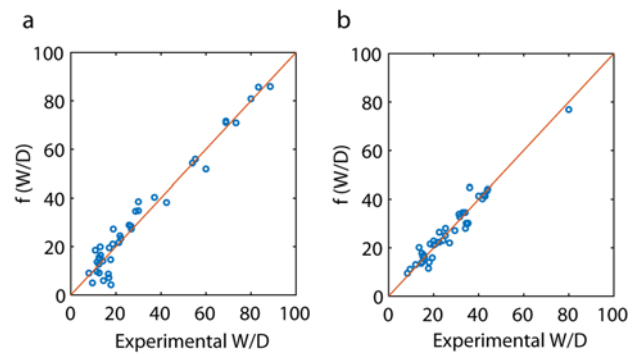


Figure 6. Estimated values vs experimental values of the parameter *W/D* for FFT method in 0-200 kHz. a) Sapphire, b) Zirconia.

According to the previous analysis, the bandwidth 0-200 kHz discretized in intervals of 10 kHz was the best methodology to obtain an optimal acoustic emission signal characterisation. This method provided an optimal correlation between the acoustic emission signal and the *W/D* parameter for both materials. The proposed method

enabled an online monitoring system to obtain the most significant information of the process from the frequency ranges of AE signals.

## V. CONCLUSIONS

In this study, the online grinding surface creation monitoring was carried out by processing the acoustic emission signals in abrasive scratch experiments. The surface creation in each scratch was assessed by using the ratio  $W/D$  of the scratch profile of maximum depth.

The TDA signal processing method failed to obtain applicable signal feature extraction for both materials. For the FFT signal processing method, the analysis of different frequency ranges with suitable selection of the bandwidth is crucial to achieve an optimal signal feature extraction that could be able to correlate the acoustic emission signals with the ratio  $W/D$ . The analysis of the frequency range of 0-600 kHz did not provide good results due to the length of the discretisation intervals (100 kHz) were too long, and the information of the AE signal could not be analysed adequately, leaving the significant information hidden or disguised in the signal appearance. The best bandwidth for acoustic emission signal relevant feature extraction was obtained at 0-200 kHz. The frequency range discretisation with intervals of 10 kHz enabled the isolation and location of signal ranges with effective information for the monitoring of the  $W/D$  parameter. Most of the 20 frequency intervals analysed in the bandwidth 0-200 kHz have a great impact indication on the  $W/D$  parameter.

Finally, the acoustic emission signal in frequency domain has proven to be an applicable signal to monitor the surface creation in abrasive scratch experiments.

## ACKNOWLEDGMENT

This research was supported by the Spanish Ministry of Education, Culture and Sport through the grant "Mobility stays abroad -José Castillejo- for young doctors" and Element Six (UK) Limited.

## REFERENCES

- [1] C. H. Lauro, L. C. Brandão, D. Baldo, R. A. Reis, and J. P. Davim, "Monitoring and processing signal applied in machining processes - A review," *Meas. J. Int. Meas. Confed.*, vol. 58, pp. 73–86, 2014.
- [2] R. Teti, K. Jemielniak, G. O'Donnell, and D. Dornfeld, "Advanced monitoring of machining operations," *CIRP Ann. - Manuf. Technol.*, vol. 59, no. 2, pp. 717–739, 2010.
- [3] A. Boaron and W. L. Weingaertner, "Dynamic in-process characterization method based on acoustic emission for topographic assessment of conventional grinding wheels," *Wear*, 2018.
- [4] A. Arun, K. Rameshkumar, D. Unnikrishnan, and A. Sumesh, "Tool Condition Monitoring of Cylindrical Grinding Process Using Acoustic Emission Sensor," in *Materials Today: Proceedings*, 2018.
- [5] M. Siddhpura and R. Paurobally, "A review of chatter vibration research in turning," *Int. J. Mach. Tools Manuf.*, vol. 61, pp. 27–47, 2012.
- [6] E. García Plaza, P. J. Núñez López, and E. M. Beamud González, "Multi-sensor data fusion for real-time surface quality control in automated machining systems," *Sensors (Switzerland)*, vol. 18, no. 12, 2018.
- [7] E. García Plaza and P. J. Núñez López, "Application of the wavelet packet transform to vibration signals for surface roughness monitoring in CNC turning operations," *Mech. Syst. Signal Process.*, vol. 98, pp. 902–919, 2018.
- [8] S. Karam and R. Teti, "Wavelet transform feature extraction for chip form recognition during carbon steel turning," *Procedia CIRP*, vol. 12, pp. 97–102, 2013.
- [9] Q. Liu, X. Chen, and N. Gindy, "Investigation of acoustic emission signals under a simulative environment of grinding burn," *Int. J. Mach. Tools Manuf.*, 2006.
- [10] Q. Liu, X. Chen, and N. Gindy, "Fuzzy pattern recognition of AE signals for grinding burn," *Int. J. Mach. Tools Manuf.*, 2005.
- [11] E. García Plaza and P. J. Núñez López, "Surface roughness monitoring by singular spectrum analysis of vibration signals," *Mech. Syst. Signal Process.*, vol. 84, pp. 516–530, 2017.
- [12] T. Warren Liao, C. F. Ting, J. Qu, and P. J. Blau, "A wavelet-based methodology for grinding wheel condition monitoring," *Int. J. Mach. Tools Manuf.*, 2007.
- [13] E. García Plaza and P. J. Núñez López, "Analysis of cutting force signals by wavelet packet transform for surface roughness monitoring in CNC turning," *Mech. Syst. Signal Process.*, vol. 98, pp. 634–651, 2018.
- [14] K. Wegener, H. W. Hoffmeister, B. Karpuschewski, F. Kuster, W. C. Hahmann, and M. Rabiey, "Conditioning and monitoring of grinding wheels," *CIRP Ann. - Manuf. Technol.*, vol. 60, no. 2, pp. 757–777, 2011.
- [15] D. T. Nguyen, S. Yin, Q. Tang, P. X. Son, and L. A. Duc, "Online monitoring of surface roughness and grinding wheel wear when grinding Ti-6Al-4V titanium alloy using ANFIS-GPR hybrid algorithm and Taguchi analysis," *Precis. Eng.*, vol. 55, no. October 2018, pp. 275–292, 2019.
- [16] J. Tang, J. Du, and Y. Chen, "Modeling and experimental study of grinding forces in surface grinding," *J. Mater. Process. Technol.*, vol. 209, no. 6, pp. 2847–2854, 2009.
- [17] D. E. Lee, I. Hwang, C. M. O. Valente, J. F. G. Oliveira, and D. A. Dornfeld, "Precision manufacturing process monitoring with acoustic emission," *Int. J. Mach. Tools Manuf.*, vol. 46, no. 2, pp. 176–188, 2006.
- [18] T. Warren Liao, "Feature extraction and selection from acoustic emission signals with an application in grinding wheel condition monitoring," *Eng. Appl. Artif. Intell.*, 2010.
- [19] N. H. Chiu and Y. Y. Guao, "State classification of CBN grinding with support vector machine," *J. Mater. Process. Technol.*, vol. 201, no. 1–3, pp. 601–605, 2008.
- [20] E. A. Dias, F. B. Pereira, S. L. M. Ribeiro Filho, and L. C. Brandão, "Monitoring of through-feed centreless grinding processes with acoustic emission signals," *Meas. J. Int. Meas. Confed.*, 2016.
- [21] G. E. P. Box, J. S. Hunter, and W. G. Hunter, *Statistics for experimenters: design, innovation, and discovery*. Wiley-Interscience, 2005.